Epoxy-Resin-Cured Carboxylated Nitrile Rubber

SUNITY K. CHAKRABORTY, and SADHAN K. DE, *Rubber Technology Center, Indian Institute of Technology, Kharagpur-721302, India*

Synopsis

Curing of carboxylated nitrile rubber (XNBR) with epoxy resin in presence of different fillers has been studied. It was observed that 7.5 phr of resin give a compromise combination of properties in FEF black (N 550)-filled vulcanizates at 40 phr loading. Further studies at different loadings of black, reinforcing silica and clay were done at 7.5 phr resin. Technical properties at different filler loadings have been determined. Polymer-filler interaction involving FEF black, silica, and clay was examined by a Kraus plot and the equation of Lorenz and Parks. Silica and carbon black give a similar type of reinforcement, but clay shows nonreinforcing characteristics. In the case of carbon black–XNBR system, polymer-filler attachment is similar to that existing in carbon black–natural rubber system. In the case of silica, reaction of the silanol group with the epoxide group of the epoxy resin and the carboxyl group of the base polymer may be responsible for the polymer-filler attachment. Scanning electron microscopy (SEM) studies of the fracture surfaces corroborate the findings on technical properties and polymer-filler interaction.

INTRODUCTION

Earlier reports of vulcanization of carboxylated nitrile rubber (XNBR) deal mostly with metal oxide (ionic crosslinking) systems.[1,2] Mixed crosslinking systems containing both ionic, and covalent sulfur–sulfur crosslinks have also been reported.[3,4] Interaction of clay and silica fillers with XNBR in a mixed crosslinking system has been studied recently.[5] One of the disadvantages of ionic systems and of mixed crosslinking systems is the scorchiness during processing and poor dynamic properties of the vulcanizates.[4] A preliminary report[1] shows that epoxy resin provides a novel crosslinking agent for XNBR. In this communication, we report results of our studies on the effect of different fillers on epoxy-cured XNBR. In the first part we have studied the effect of varying concentrations of resin on FEF black (N 550)-filled XNBR at two different curing temperatures (150°C and 180°C), and in the second part we have studied the effect of varying loadings of FEF black, reinforcing silica, and clay on XNBR at constant resin concentration (7.5 phr) and at one curing temperature (180°C). In the third part, we report results of our SEM studies on the tensile and tear fracture surfaces of epoxy-cured XNBR composites.

EXPERIMENTAL

Formulations of the mixes are given in Table I. Mixing was done in a conventional laboratory mill (15 cm × 33 cm) at 30–40°C, according to ASTM D15-70. Mixes were vulcanized at 150°C and 180°C at their respective optimum cure times as obtained from Monsanto Rheometer R-100. On removal from the mold, the vulcanizates were cooled quickly in water at the end of the curing cycle. Testing procedures were described earlier.[6] In some mixes rheographs were

Journal of Applied Polymer Science, Vol. 27, 4561–4576 (1982)
 CCC 0021-8995/82/124561-16$02.60

TABLE I
Formulations of the Mixes

Mix	A_1	A	B	C	D	E	F
KRYNAC 221[a]	100	100	100	100	100	100	100
Stearic acid	2	2	2	2	2	2	2
FEF black (N 550)[b]	40	40	40	40	40	40	40
Epoxy resin[c]	3.0	5.0	7.5	10.0	12.5	15.0	20.0

[a] Highly carboxylated nitrile rubber with medium acrylonitrile content. Obtained from Polysar Limited, Canada, ML(1 + 4) at 100°C, 50; total ash content, 0.77%; nonstaining antioxidant; specific gravity, 0.98.

[b] Carbon black obtained from Phillips Carbon Black Ltd., Durgapur.

[c] Grade LY 553, Diglycidylether of bisphenol A obtained from CIBATUL Ltd., Bombay.

taken at two different curing temperatures and the rate constants were determined[7] by plotting $\log(R_\infty - R_t)$ against time (t), where the constant R_∞ corresponds to the maximum rheometric torque and R_t is the torque at time t. The first-order rate constant was determined from the negative slope of the straight line portion of the curve obtained beyond the induction period. The activation energy was calculated from rate constant values at two different temperatures using Arrhenius equation.

In the present work we have determined V_r (volume fraction of rubber in the

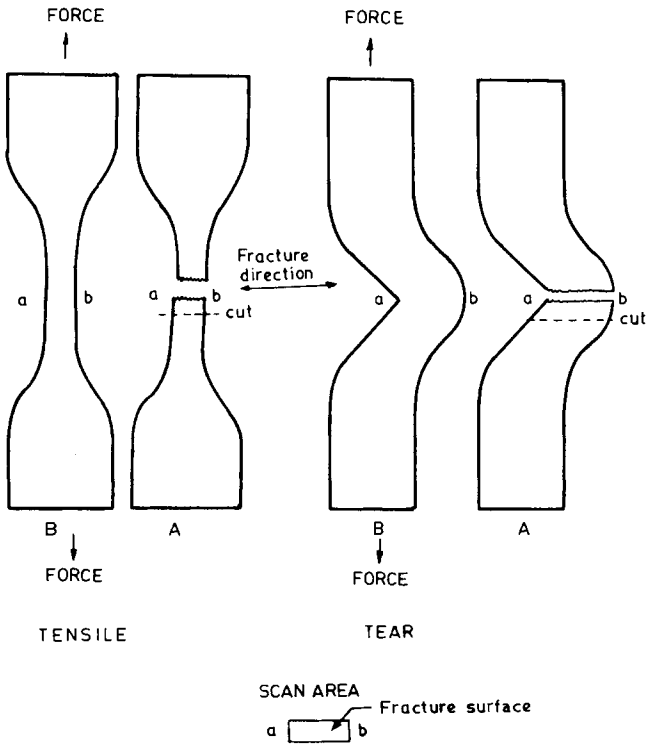

Fig. 1. Tear and tensile specimens with fracture direction and scan area: (B) before testing; (A) after testing.

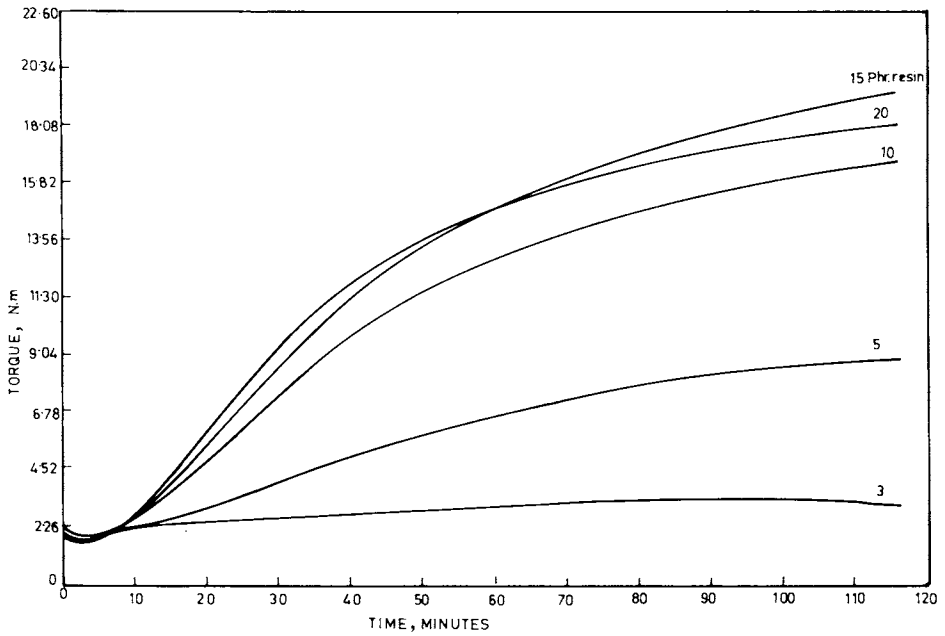

Fig. 2. Rheographs of mixes A_1, A, C, E, and F (Table I) at different resin loadings at 150°C.

swollen vulcanizate) by assuming that filler does not swell. V_r can be taken as a measure of crosslink density. Swelling was done in chloroform at 35°C for 36 h when equilibrium was achieved. V_r was calculated as

$$V_r = \frac{(D - FT)\rho_r^{-1}}{(D - FT)\rho_r^{-1} + A_0\rho_s^{-1}} \tag{1}$$

where T is the weight of the test specimen, D, the deswollen weight of the test specimen, F, the weight fraction of insoluble components of the vulcanizate, A_0, the weight of the absorbed solvent and corrected for the swelling increment, and ρ_r and ρ_s are the densities of the rubber and the solvent respectively (ρ_s = 1.48 for chloroform and ρ_r = 0.98 for XNBR). A modified preswelling procedure,[8] which was designed to chemically break polymer–filler bonds in case of silicone rubber, ethylene propylene, and polybutadiene rubbers, was used in XNBR in the present study in order to determine the contribution of polymer–silica filler attachments on the effective number of chemical crosslinks. The samples were swollen for 48 h in chloroform exposed to ammonia atmosphere in order to break the polymer–filler attachments. The volume fraction of rubber (V_r) of the ammonia-treated vulcanizates was determined as described earlier.

The SEM observations of the tensile and tear fracture surfaces were made using a Philips 500 model scanning electron microscope. After the testing, fracture surfaces of the test specimens were carefully cut out from one of the two pieces of the failed test specimens without touching the surface. The fractured surfaces were then sputter-coated with gold within 24 h of testing. The tilt was adjusted at 0°, and the orientation of the photographs was kept the same in all cases. Figure 1 shows details of the test specimens, fracture direction, and scan area.

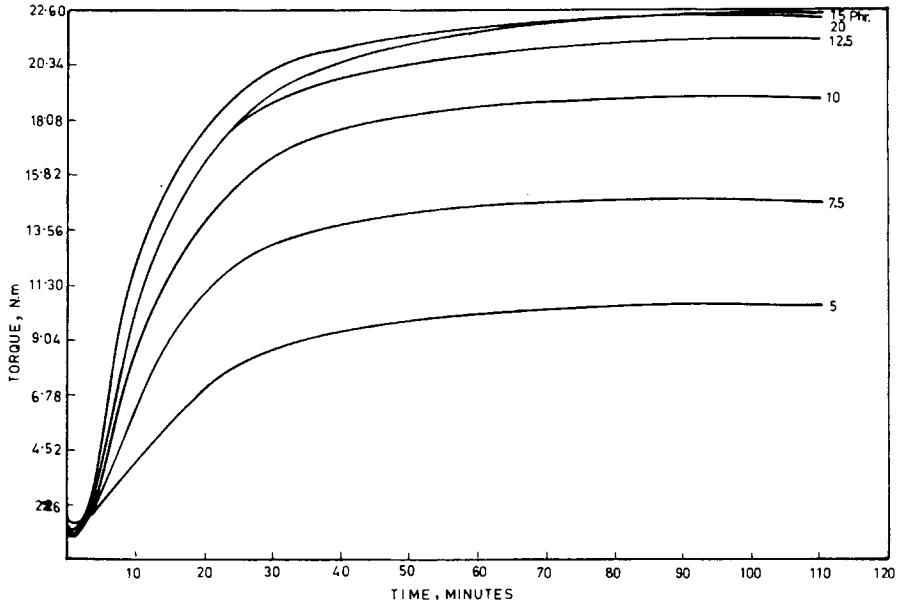

Fig. 3. Rheographs of mixes A–F (Table I) at different resin loadings at 180°C.

RESULTS AND DISCUSSION

Effect of Resin Content on FEF Black-Filled XNBR

In all cases mixing was smooth and uniform. Rheographs at two different temperatures (150°C and 180°C) are shown in Figures 2 and 3. Curing characteristics are reported in Table II. A rheograph shows that 3 phr resin is not sufficient for curing. An increase in resin content increases the rheometric maximum torque and lowers the Mooney viscosity, showing that the resin acts as a processing aid during mixing and as a curing agent during vulcanization. The scorch time decreases fast beyond 7.5 phr of resin. However, the optimum cure time drops only marginally. Maximum rheometric torque increases with increase in resin concentration till 15 phr, indicating increase in crosslink density. But, at 20 phr loading, the maximum torque decreases, showing plasticizing action at higher resin concentration.

TABLE II
Curing Characteristics of the Mixes Using Mooney Viscometer and Monsanto Rheometer (R-100)

Mix	A	B	C	D	E	F
Mooney no. ML(1 + 4) at 120°C	49	42	40	38	36	32
Mooney scorch time t_5 at 120°C (min)	45	42	22	20	18	17
Optimum cure time (min)						
(a) At 180°C	29.0	27.5	27.5	27.0	27.0	25.0
(b) At 150°C	68.0	—	55.0	—	52.0	45.0

TABLE IIIA
Physical Properties of the Vulcanizates Cured at 150°C

Mix	A	C	E	F
Tensile strength (MPa)	16.36	19.39	16.27	15.43
Modulus at 100% elongation (MPa)	1.62	3.81	4.50	4.54
Elongation at break (%)	586	320	270	230
Tear strength (kN/m)	38.85	25.32	17.98	17.04
Hardness, Shore A	70	72	74	85
Resilience (%)	41	48	49	49
Heat buildup (ΔT°C)	50.0	26.5	22.0	18.5
Permanent set (%)	4.9	0.4	0.2	0.2
Compression set (%)	24	16	16	20
Flex cracking at 70°C up to failure (kcycles)	64.17	4.43	1.00	0.77
Abrasion loss (cm^3/1000 revolutions)	0.90	1.02	1.20	1.11
Volume fraction of rubber (V_r)	0.124	0.188	0.202	0.204

Technical properties of the FEF black-filled mixes at varying resin contents cured at 150°C and 180°C are summarized in Tables IIIA and IIIB. The curing reaction of epoxy resin with carboxylated nitrile rubber is shown in Figure 4. Higher modulus, lower elongation at break, lower tear strength, higher resilience, and lower heat buildup at higher resin content show increasing tightness of cure with increase in resin content. This is also evident from increase in V_r, volume fraction of rubber in the swollen vulcanizate, and maximum rheometric torque as discussed earlier. Examination of curing characteristics and technical properties shows that 7.5 phr loading of epoxy resin is an optimum concentration for obtaining a compromise set of processing and technical properties. Comparison of physical properties of vulcanizates cured at 150°C and 180°C shows that higher curing temperature does not have much detrimental effect on properties. Similar observations in case of mixed crosslinking system have been made earlier by Bhowmick and De.[3]

In the following section, we study technical properties and polymer–filler interaction of XNBR vulcanizates cured at 180°C containing FEF black, silica, and clay at 7.5-phr resin concentration.

TABLE IIIB
Physical Properties of the Vulcanizates Cured at 180°C

Mix	A	B	C	D	E	F
Tensile strength (MPa)	16.46	17.28	16.88	14.60	14.05	11.96
Modulus at 100% elongation (MPa)	1.54	2.29	3.72	4.81	5.11	5.75
Elongation at break (%)	480	365	260	200	188	160
Tear strength (kN/m)	35.52	31.91	29.52	18.67	16.77	11.51
Resilience (%)	41	44	47	48	52	53
Abrasion loss (cm^3/1000 revolutions)	0.85	0.88	1.04	1.08	1.16	1.31
Hardness, shore A	65	70	74	78	78	85
Compression set (%)	18	12	12	7	7	6
Permanent set (%)	1.4	0.6	0.2	0.1	0.1	0.1
Flex cracking at 70°C, up to failure (kcycles)	58.03	4.27	0.55	0.23	0.20	0.10
Heat buildup (Δ T°C)	42.5	31.0	26.0	20.5	15.5	12.5
Volume fraction of rubber (V_r)	0.171	0.196	0.219	0.262	0.264	0.277

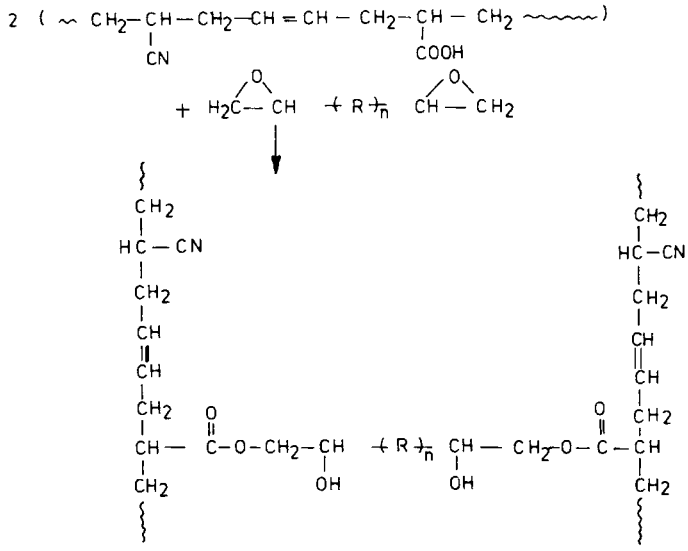

Fig. 4. Crosslinking reaction of carboxylated Nitrile rubber by epoxy resin.[1]

Technical Properties and Polymer-Filler Interaction of Epoxy-Resin-Cured XNBR

Formulations of the mixes are given in Table IV. Rheographs of different mixes are shown in Figures 5–7. The maximum rheometric torque, as expected, increases with increase in black loading but the trend is the reverse in the case of clay. In the case of silica filler, it increases up to 10 phr loading and then decreases at higher filler loadings. But the minimum rheometric torque, as expected, increases continuously with increase of filler loadings in all cases. Table V gives the processing characteristics of some of the mixes in presence and absence of epoxy resin. The addition of resin lowers the Mooney number and minimum viscosity. It shows that epoxy resin in filled carboxylated nitrile rubber acts as a processing aid at processing temperature and as a curing agent at curing temperature (Fig. 4). Mooney scorch time values show that resin curing gives better scorch safety as compared to ionic and mixed crosslinking systems.[3–5]

Silica is likely to undergo bonding with epoxy resin, because silanol groups present in silica filler are susceptible to reaction with carboxyl groups in XNBR and epoxide groups in epoxy resin. It has been shown by Edward and Sato[9] that the epoxy group can react with silanol groups of silica filler and provide polymer–filler attachment.

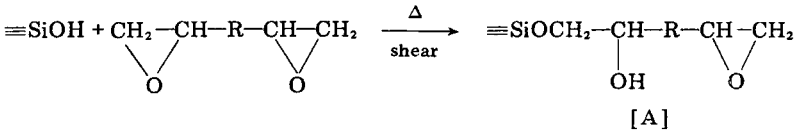

(2)

[A]

[A] can react with the carboxyl group in XNBR and with silica during milling and curing to give polymer–filler and filler–filler attachments.

TABLE IV
Formulations of the Mixes

Mix	Gum	B_{10}	B_{20}	B_{40}	B_{60}	G_{10}	G_{25}	G_{40}	G_{60}	H_{15}	H_{35}	H_{60}	H_{80}
KRYNAC 221	100	100	100	100	100	100	100	100	100	100	100	100	100
Stearic acid	2	2	2	2	2	2	2	2	2	2	2	2	2
FEF (N 550)	—	10	20	40	60	—	—	—	—	—	—	—	—
Silica[a]	—	—	—	—	—	10	25	40	60	—	—	—	—
Clay[b]	—	—	—	—	—	—	—	—	—	15	35	60	80
Epoxy resin	7.5	7.5	7.5	7.5	7.5	7.5	7.5	7.5	7.5	7.5	7.5	7.5	7.5

[a] Vulcasil-S obtained from Bayer (India) Ltd., Bombay.
[b] Soft clay obtained from Dunlop (India) Ltd., Sahaganj (pH of the slurry = 4.5).

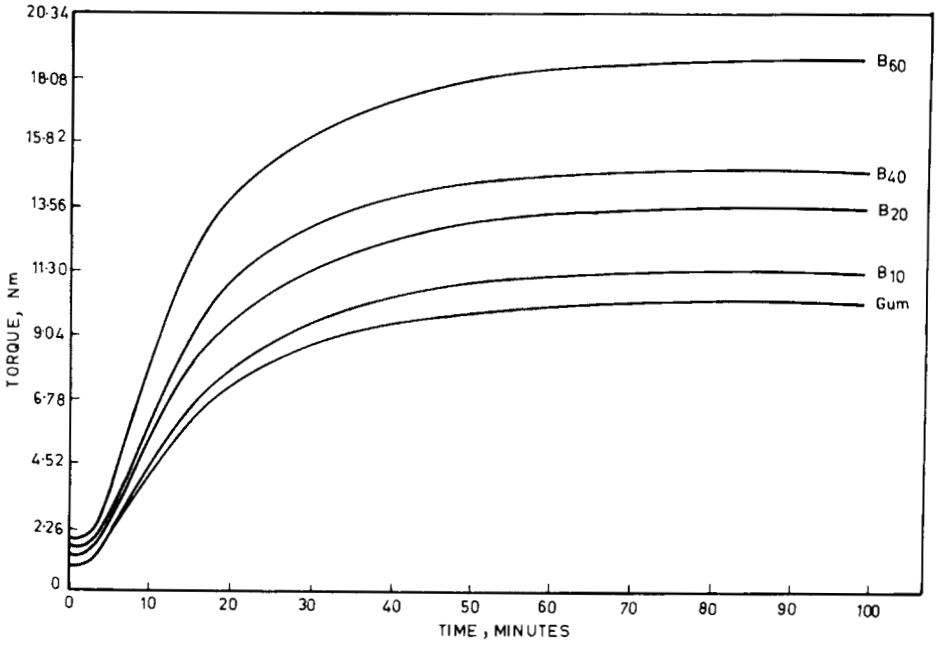

Fig. 5. Rheographs of mixes gum, B_{10}–B_{60} (Table IV), at different black loadings at 180°C.

$$[A] + HO{-}\overset{\overset{O}{\|}}{C}{-}P \xrightarrow[\text{shear}]{\Delta} \equiv SiOCH_2{-}\underset{OH}{CH}{-}R{-}\underset{OH}{CH}{-}CH_2{-}O{-}\overset{\overset{O}{\|}}{C}{-}P \qquad (3)$$

$$\equiv SiOH + [A] \xrightarrow[\text{shear}]{\Delta} \equiv SiOCH_2{-}\underset{OH}{CH}{-}R{-}\underset{OH}{CH}{-}CH_2OSi{\equiv} \qquad (4)$$

Also, silanol groups can react with carboxyl groups in polymer chain,

$$\equiv SiOH + HO{-}\overset{\overset{O}{\|}}{C}{-}P \xrightarrow[\text{shear}]{\Delta} Si{-}O{-}\overset{\overset{O}{\|}}{C}{-}P \qquad (5)$$

Another possible reaction between silica and carboxyl groups involve divalent metal ion:

$$\equiv SiOH + M^{++} + HO{-}\overset{\overset{O}{\|}}{C}{-}P \longrightarrow \equiv Si{-}O{-}M{-}O{-}\overset{\overset{O}{\|}}{C}{-}P \qquad (6)$$

where M stands for Ca, Mg, etc., present in silica (or clay) and P signifies a polymer chain.

Decrease in maximum rheometric torque and increase in minimum rheometric torque[10] with increase in silica loading is possibly due to polymer–filler bonding and filler–filler bonding, thereby effectively removing epoxy resin from the polymer and depressing crosslink formation. Activation energy values of gum and black-filled (mix B_{40}) mixes are the same (that is, 59 kJ/mol), indicating no

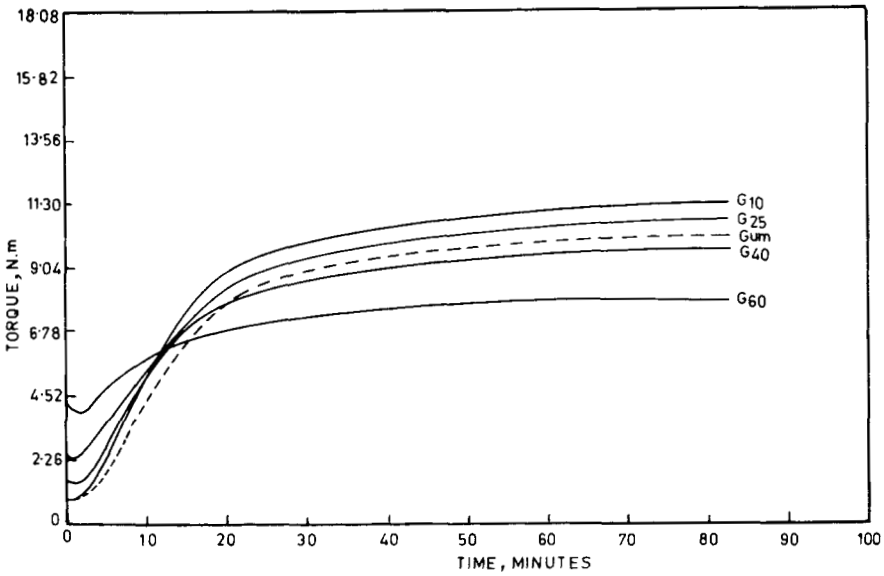

Fig. 6. Rheographs of mixes gum, G_{10}–G_{60} (Table IV), at different silica loadings at 180°C.

detectable effect of carbon black on vulcanization. In the case of silica-filled and clay-filled compounds, activation energy values are higher (mix G_{40}, 65 kJ/mol, and mix H_{60}, 70 kJ/mol). This indicates the effects of silica and clay on vulcanization.

The polymer–filler interaction was analyzed by the Kraus equation[11]:

$$V_{r0}/V_{rf} = 1 - m\phi/(1 - \phi) \tag{7}$$

$$m = 3C(1 - V_{r0}^{1/3}) + V_{r0} - 1 \tag{8}$$

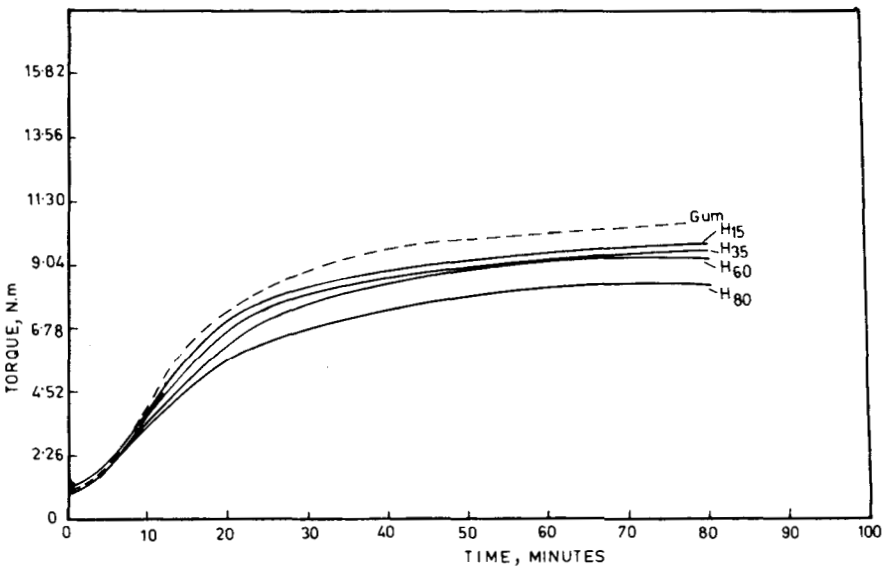

Fig. 7. Rheographs of mixes gum, H_{15}–H_{80} (Table IV), at different clay loadings at 180°C.

TABLE V
Processing Characteristics of the Mixes[a]

Mix	B_{40} (black-filled)	G_{40} (silica-filled)	H_{60} (clay-filled)
Mooney no. ML (1 + 4) at 120°C	42 (53)	68 (88)	34 (42)
Minimum viscosity	43 (50)	68 (80)	32 (39)
Mooney scorch time t_5 (min)	42	17	34

[a] Values in parenthesis are the results of mixes without resin.

Here V_{r0} represents the volume fraction of rubber in the gum vulcanizate, V_{rf} is the volume fraction of rubber in the filled vulcanizate, C is a constant characteristic of filler but independent of the polymer, the solvent, and the degree of vulcanization and ϕ is the volume fraction of filler in the filled vulcanizate. Figure 8 shows the Kraus plots for different fillers. Silica and black fillers follow the Kraus equation and show similar reinforcement, but clay shows abnormal behavior due to lack of polymer–filler attachment. Clay causes the onset of dewetting and vacuole formation, no longer fulfiling the condition set forth in the Kraus theory. At lower clay loadings, the system is nonadherent, becoming weakly adherent only at higher concentration. SEM studies, described later, confirm those observations. Whiting also behaved abnormally in respect to Kraus plots, as reported earlier in case of natural rubber.[12] The extent of reinforcement was further analyzed by the equation of Lorenz and Parks[13]:

$$Q_f/Q_g = a \cdot e^{-z} + b \tag{9}$$

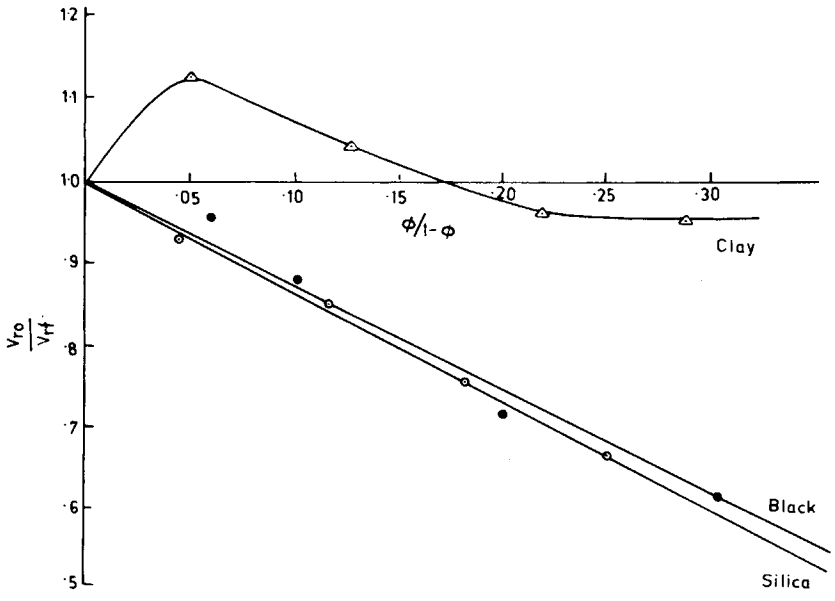

Fig. 8. Kraus plots according to eq. (7).

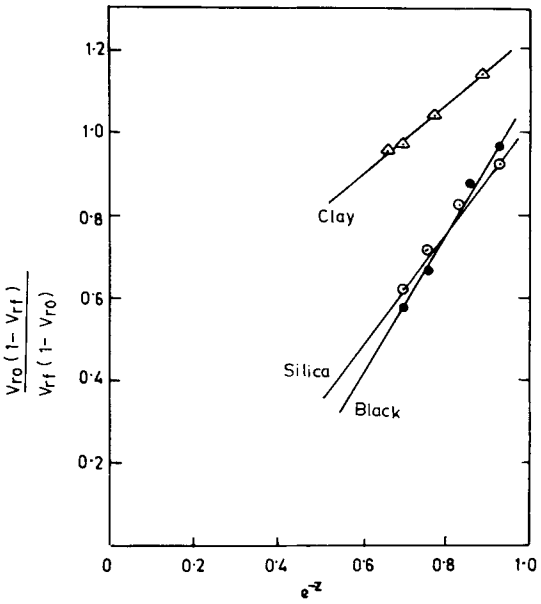

Fig. 9. Lorenz and Parks plots according to eq. (10).

or

$$\frac{V_{r0}(1 - V_{rf})}{V_{rf}(1 - V_{r0})} = a \cdot e^{-z} + b \tag{10}$$

where Q is the amount of solvent imbibed per unit weight of the rubber, f and g refer to filled and gum mixes, and z is the ratio by weight of filler to rubber in the rubber vulcanizate. V_{r0} and V_{rf} are the volume fractions of rubber in gum and filled vulcanizates, respectively, swollen in a solvent. The constants a and b are characteristic of the system. Figure 9 shows the plots of $V_{r0}(1 - V_{rf})/V_{rf}(1 - V_{r0})$ vs. e^{-z}, wherein we find that silica and black fillers show similar extent of reinforcement and reinforcing activity of clay is less [a values of eq. (10): for FEF black 1.75, for silica 1.43, for clay 0.82].

Technical properties of the vulcanizates at varying filler loadings are given in Table VI. In the case of black- and silica-filled vulcanizates, tensile strength, modulus, hardness, and tear strength increase and resilience decreases with increase in filler loading. The effect is less pronounced in the case of clay. Increase of elongation at break along with tensile strength with the addition of silica filler is due to increased mobility, higher interaction of filler, and low state of cure, as discussed earlier, which allows the elastomer chains to slip over the silica surface.[5,12] It appears that polymer–filler interaction in the case of carbon black–XNBR systems vulcanized by epoxy resin is similar to the carbon black–natural rubber system. The presence of pendent —COOH group does not play an extra role in the polymer–filler attachment. SEM photomicrographs, as described below, show that fracture surfaces of black-filled XNBR is similar to that of black-filled NR[16]. But in the case of silica, polymer-filler attachment is mainly due to reactions (2)–(6). In the case of silica-filled systems, results of V_r after ammonia treatment (Table VI) are the same as that of gum V_r, indi-

TABLE VI
Characterization of the Vulcanizates at Different Filler Loadings

Mix	Gum	B_{10}	B_{20}	B_{40}	B_{60}	G_{10}	G_{25}	G_{40}	G_{60}	H_{15}	H_{35}	H_{60}	H_{80}
Optimum cure time, at 180° (min)	29.0	28.0	27.5	27.5	27.0	25.0	25.0	25.0	16.0	26.0	28.0	29.0	30.0
Tensile strength (MPa)	0.74	4.55	9.29	17.28	20.27	3.42	6.47	14.73	14.13	2.59	6.14	8.72	9.55
Modulus at 100% elongation (MPa)	0.10	1.37	1.89	2.29	11.70	1.38	1.84	3.56	4.50	1.40	1.90	2.80	3.44
Elongation at break (%)	350	430	400	365	250	400	440	700	710	500	610	650	700
Hardness, Shore A	50	52	56	70	80	52	60	65	70	50	54	62	65
Tear strength (kN/m)	3.19	10.25	14.13	31.91	32.18	9.70	22.40	38.85	43.95	4.47	11.04	14.98	34.30
Resilience (%)	46	45	45	44	41	41	40	39	39	42	43	43	43
V_r (volume fraction of rubber)	0.139 (0.139)[a]	0.144 —	0.158 —	0.196 —	0.221 —	0.149 (0.146)	0.165 (0.149)	0.184 (0.148)	0.206 (0.138)	0.124 —	0.133 —	0.143 —	0.144 —

[a] Values in the parenthesis are the V_r measured over ammonia atmosphere.

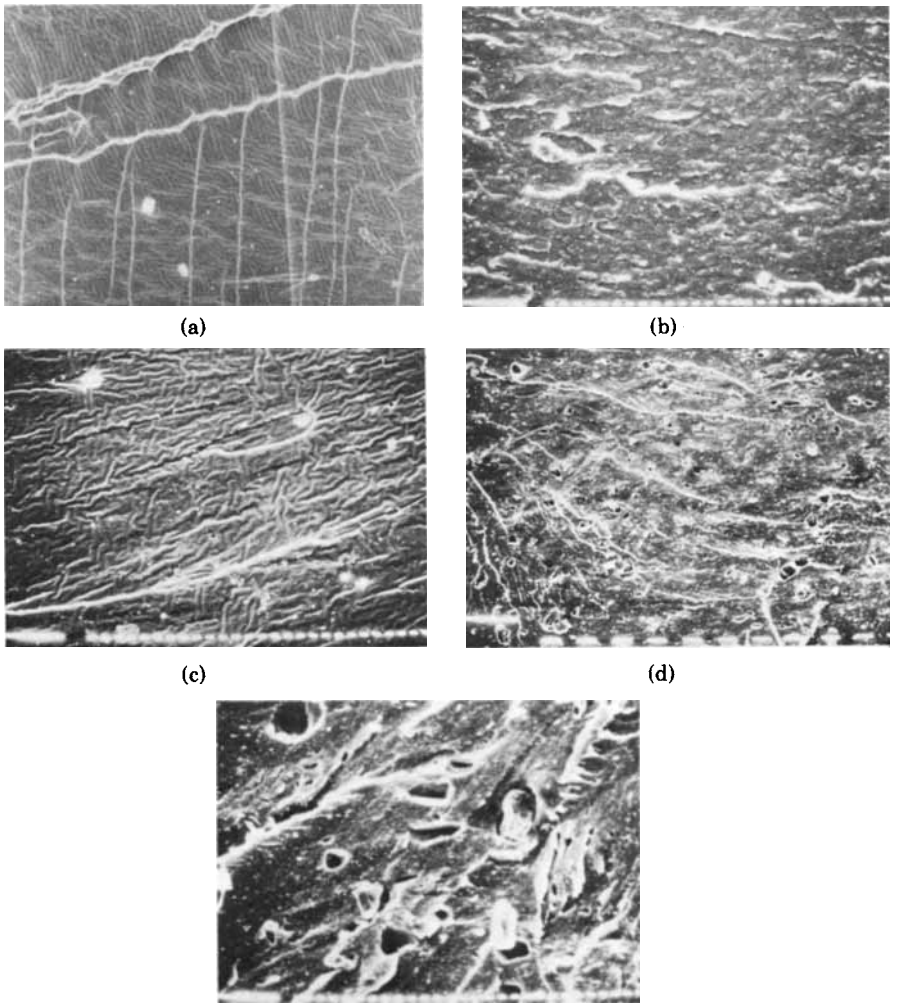

Fig. 10. SEM photomicrographs of tensile fractured surfaces: (a) tear lines and ripplings on the surface (gum mix) (60 ×); (b) rough surface with short and rounded tear lines (black filler, mix B_{40}) (50 ×); (c) short tear lines with ripplings on the surface (silica filler, mix G_{40}) (200 ×); (d) pitted surface with scattered tear lines (clay filler, mix H_{60}) (50 ×); (e) detached clay agglomerates (mix H_{60}) (200 ×).

cating formation of polymer–filler attachments through active groups which disintegrate on ammonia treatment. However, in the case of clay-filled mixes, V_r values are less than that of silica-filled mixes, indicating lack of polymer–filler attachment. V_r values of carbon-black-filled vulcanizates are similar to that of silica-filled vulcanizates. This is in conformity with the results of Kraus plots and Lorenz and Parks[13] plots.

SEM Studies of Tensile and Tear-Fractured Surfaces

Tensile and tear-fractured surfaces were studied by SEM. Recently, SEM has been used as a tool to study the fracture characteristics of rubber vulcani-

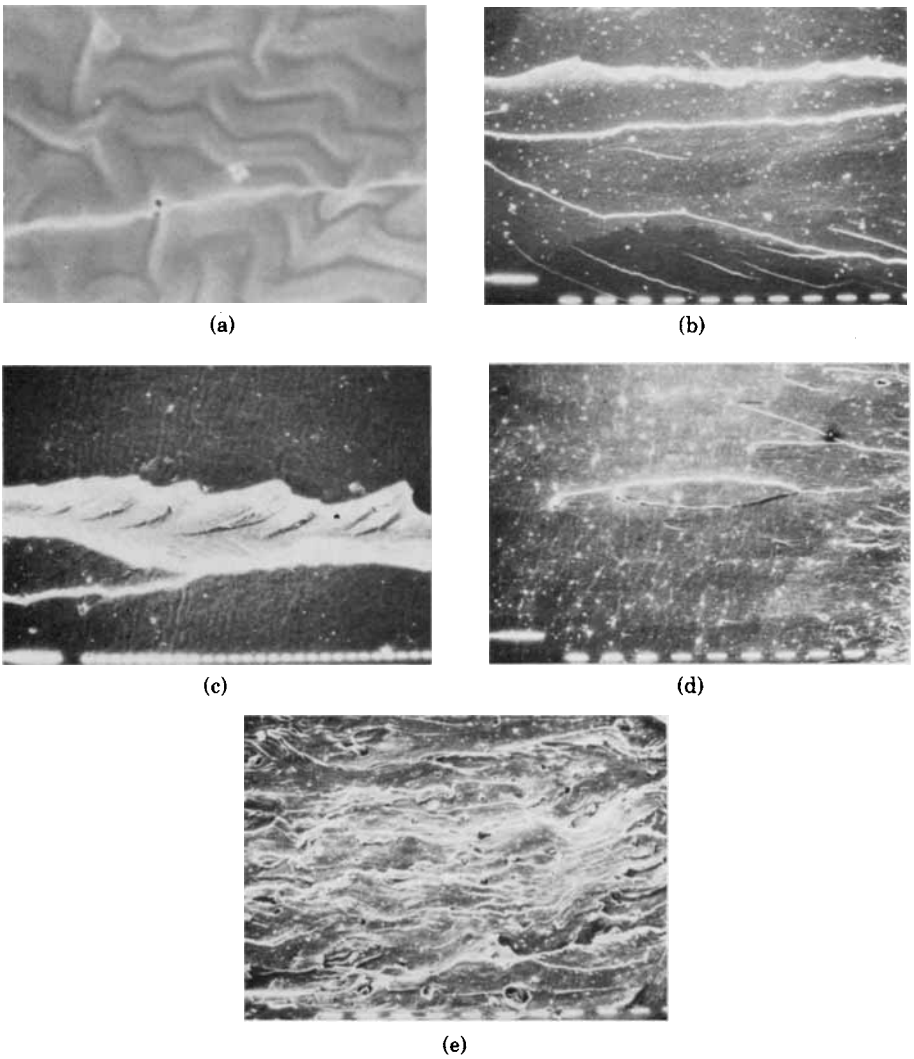

Fig. 11. SEM photomicrographs of tear fractured surfaces: (a) surface ripplings with steady tear line (mix gum) (400 ×); (b) short, steady tear, and stick-slip type tear (black filler, mix B_{40}) (50 ×); (c) details of one primary tear path (mix B_{40}) (200 ×); (d) short tear lines and surface ripplings (silica filler, mix G_{40}) (50 ×); (e) tear paths and detached clay agglomerates on the surface (clay filler, mix H_{60}) (50 ×).

zates.[14–16] In the earlier sections of this paper we observed that silica and carbon black show similar reinforcement. However, silica reacts with the polymer (XNBR) as well as the curing agent (epoxy resin), but carbon black has no detectable effects on vulcanization of the XNBR by the epoxy resin. Clay affects the vulcanization, but shows nonadherence with the polymer. Fracture topography of the tensile specimens provides support for some of these observations.

SEM photomicrographs of tensile fractured surfaces are shown in Figures 10(a)–(e). Figure 10(a) shows the photomicrograph of gum vulcanizates. The fractured surface shows smooth tear lines perpendicular to the direction of stress.

Secondary tear lines or branches were perpendicular to the direction of the primary tear lines, and fine ripplings were visible on the surface. In the case of the mixed crosslinking system,[5] tear lines were shorter, no branches were formed, and the strength was also higher. The addition of fillers changes the fracture pattern [Fig. 10(b)]. The enhancement of the tensile strength was observed with the addition of black filler. The rippling and smooth tear lines were replaced by rough surface consisting of curved short tear paths. In the case of natural rubber also, we observed similar fracture surface.[16] The tear lines are believed to be arrested or deviated by the filler particles in these systems. Addition of silica in epoxy-cured polar XNBR raises the surface energy[17] and results in improved adhesion and wetting characteristics, as discussed earlier. SEM photomicrograph [Fig. 10(c)] shows better adhesion. In fact, the surface is similar to gum vulcanizate. But the secondary tear lines (or branches) were not visible and the tear lines were shorter. In the case of the mixed crosslinking system of XNBR[5] and in the sulfur curing system of NR,[18] the silica-filled vulcanizate surface showed silica aggregates on the fracture surface. No such aggregate was observed here. This is due to the efficient bonding between polymer and filler. The addition of clay in epoxy-cured XNBR changes the fracture mode remarkably, as seen in photomicrographs 10(d) and 10(e). The fracture surface is rough with discontinuous tear lines. The small pits which appear on the surface is due to debonding of clay-filler from the polymer matrix.

Figures 11(a)–(e) show the SEM photomicrographs of tear-fractured surface of epoxy cured XNBR vulcanizates. Figure 11(a) shows surface ripplings and a steady tear line similar to sulfur-metal oxide-cured XNBR gum vulcanizate.[5] The addition of black changes the fracture mode from steady tear to stick-slip tear [Figs. 11(b) and 11(c)] with increase in tear resistance.[19] In the case of silica-filled vulcanizate the obstruction of tear path results from better silica-polymer adhesion [Fig. 11(d)], which arrest the growth of tear tip diameter.

In the case of clay-filled XNBR, the tear paths proceed from one end to the other. The interaction of clay with XNBR is weak as reported earlier. Photomicrograph 11(e) shows a large number of pits on the surface. The formation of a large number of pits on the surface is due to detachment of clay agglomerates from the polymer matrix.

References

1. H. P. Brown, *Rubber Chem. Technol.*, **36,** 931 (1963).
2. D. C. Coulthard, K. Ritchie, and J. Walker, paper presented at a meeting of the Rubber Division, A.C.S., San Francisco, 1976.
3. A. K. Bhowmick and S. K. De, *Rubber Chem. Technol.*, **53,** 107 (1980).
4. S. K. Chakraborty, A. K. Bhowmick, and S. K. De, *J. Appl. Polym. Sci.*, **26,** 4011 (1981).
5. S. K. Chakraborty and S. K. De, *Rubber Chem. Technol.*, **55,** Sept./Oct. (1982).
6. R. Mukhopadhyay, S. K. De, and S. N. Chakraborty, *Polymer*, **18,** 1243 (1977).
7. A. Y. Coran, *Rubber Chem. Technol.*, **38,** 1 (1965).
8. K. E. Polmanteer and C. W. Lentz, *Rubber Chem. Technol.*, **48,** 795 (1975).
9. D. C. Edwards and K. Sato, *Rubber Chem. Technol.*, **52,** 263 (1979).
10. B. B. Boonstra, H. Cochrane, and E. M. Dannenberg, *Rubber Chem. Technol.*, **48,** 558 (1975).
11. G. Kraus, *J. Appl. Polym. Sci.*, **7,** 861 (1963), and *Rubber Chem. Technol.*, **37,** 6 (1964).
12. R. Mukhopadhyay and S. K. De, *Rubber Chem. Technol.*, **52,** 263 (1979).
13. O. Lorenz and C. R. Parks, *J. Polym. Sci.*, **50,** 299 (1961).

14. S. K. Chakraborty, A. K. Bhowmick, S. K. De, and B. K. Dhindaw, *Rubber Chem. Technol.*, **55,** 41 (1982).
15. D. K. Setua, S. K. Chakraborty, S. K. De, and B. K. Dhindaw, *J. Scanning Electron. Microsc.*, to appear.
16. N. M. Mathew and S. K. De, *Polymer*, **23,** 632 (1982).
17. J. R. Creasey, D. B. Russell, and M. P. Wagner, *Rubber Chem. Technol.*, **41,** 1300 (1968).
18. V. M. Murty and S. K. De, *Rubber Chem. Technol.*, **55,** 287 (1982).
19. J. Glucklick and R. F. Landel, *J. Appl. Polym. Sci.*, **20,** 121 (1976).

Received September 11, 1981
Accepted June 11, 1982